Bi-GRU Enhanced Cost-Effective Memory-Aware End-to-End Learning for Geometric Constellation Shaping in Optical Coherent Communications

Zhiyang Liu, Xiaoyu Liu, Shilin Xiao, Weiying Yang, and Weisheng Hu

***Abstract*—We propose a cost-effective and memory-aware end-to-end learning scheme utilizing bi-directional gated recurrent unit (bi-GRU) for geometric constellation shaping (GCS) under the first-order regular perturbation (FRP) auxiliary channel. The performance of the proposed system has been numerically verified at a 32 GBd 5-channel wavelength division multiplexing (WDM) 64 quadrature amplitude modulation (QAM) 800 km optical coherent communication system. Results show that the proposed bi-GRU based GCS scheme can achieve a performance gain over square 64QAM in mutual information (MI) with 0.12 bits/symbol and a Q-factor gain of 0.4 dB at optimal launched optical power. When transmission distance is extended to 1280 km, a generalized mutual information (GMI) gain of 0.136 bits/symbol is observed. Additionally, compared with the bi-directional long short-term memory (bi-LSTM) based GCS, the proposed bi-GRU scheme has lower computation complexity with similar system performance.**

***Index Terms*—Bi-directional gated recurrent unit, end-to-end learning, geometric constellation shaping.**

I. Introduction

RAPIDLY growing demand for higher spectral efficiency (SE) in the standard single mode fiber (SSMF) promotes the integration of wavelength division multiplexing (WDM) and high-order modulation. Under a given WDM system setting, modulation format optimization is an effective approach to further increase the SE, namely probabilistic or geometric constellation shaping. Probabilistic constellation shaping (PCS), known for its rate adaptivity [1], may be incompatible with high-speed hardware implementation due to conventional serial distribution matcher [2]. However, geometric constellation shaping (GCS) provides an alternative by directly optimizing the constellation points to circumvent the serial calculation in distribution matchers.

In order to further facilitate and optimize the design of constellations in GCS, machine learning based technique was introduced. As proposed in [3], [4], the conventional transceiver block structure in typical optical communication systems could be entirely replaced by an end-to-end (E2E) learning-based autoencoder (AE) structure. In [5], the E2E fashion was utilized to compute achievable information rates under a simplified fiber channel, showing robustness to nonlinear phase noise and performance improvement. There has been a growing research attention for E2E learning facilitated GCS schemes in optical communication systems [6], [7], [8], [9]. GCS was firstly integrated with E2E learning using mutual information (MI) as performance metric in [6] and E2E learning aided GCS regarding fiber nonlinearity has been carried out in [7]. In order to accommodate the bit-wise system design, the performance metric of generalized mutual information (GMI) was introduced for E2E learned GCS structure in [8], [9]. MI and GMI can be estimated using the corresponding decoder neural networks (NN), which further evaluates the system capacity gain [6], [8]. In E2E learned GCS, the auxiliary channel model also plays an important role since the training procedure is often gradient-based backpropagation. In [10] the split-step Fourier method (SSFM) for fiber channel modeling was embedded in the E2E learning network structure to achieve SE gains in long-haul coherent optical communication. Nevertheless, simulations of long-haul WDM system with nonlinear effects are cumbersome using SSFM. Consequently, the appropriate and accurate differentiable modeling of fiber-optic channel is imperative for cost-effective and memory-aware emulations of the WDM system. Modeling of such systems in differentiable channels can provide more efficient analysis in E2E AE structures. Various differentiable auxiliary channel modeling methods have been proposed. The Gaussian noise (GN) model measures the nonlinear interference in the channel as memoryless additive white Gaussian noise (AWGN) related to launch power, but nonlinear effects are not mitigated [11]. The nonlinear interference noise (NLIN) approach further includes the modulation dependent effects, mitigating nonlinear effects by optimizing its high-order moments [7], [12]. However, channel memory, such as inter-symbol interaction, is neglected in both GN and NLIN auxiliary models. Thereafter, first-order regular perturbation (FRP) auxiliary channel model is proposed, using the first-order polynomial approximation of the nonlinearity to simulate the channel memory in the fiber-optic channel [13].

In terms of neural network in E2E learning GCS, most previous studies are based on layers of feed-forward neural network

Manuscript received 13 December 2023; accepted 15 December 2023. Date of publication 18 December 2023; date of current version 3 January 2024. The work was supported in part by the National Nature Science Fund of China under Grants 62071295 and 61775137, and in part by the National "863" Hi-Tech Project of China. *(Corresponding author: Shilin Xiao.)*

The authors are with the State Key Laboratory of Advanced Optical Communication Systems and Networks, Shanghai Jiao Tong University, Shanghai 200240, China (e-mail: dextermorgen@sjtu.edu.cn; lxiaoyu@sjtu.edu.cn; slxiao@sjtu.edu.cn; ywy_will@sjtu.edu.cn; wshu@sjtu.edu.cn).

Digital Object Identifier 10.1109/JPHOT.2023.3344184

(FFNN), which are unable to compensate for fiber chromatic dispersion (CD) and nonlinearity mixed effects. Therefore, to emulate the channel memory feature in optical coherent WDM systems, optimizations in both transceiver design and memory-aware auxiliary channel modeling are considered. Firstly, for the transceiver design, the recurrent neural network (RNN) based E2E learning scheme can provide performance gains in comparison to block-based schemes due to its sequential learning ability. However, vanilla RNN is prone to gradient vanishing or explosion, causing possible difficulties in the E2E training process [14]. Moreover, RNNs can have difficulty learning long-term dependencies, which means that they may not be able to remember information from earlier in the sequence when making predictions later on. Therefore, RNNs may not be able to capture complex patterns. To deal with the inherent flaws of RNN, the long short-term memory network (LSTM) [15] and gated recurrent unit (GRU) [16], were proposed with advanced long-term learning capabilities. In [17], LSTM and GRU were proved effective as fiber nonlinearity equalizers, but the performance improvement in LSTM models comes with high complexity. To exploit the sequential feature from the neighboring samples, bi-directional RNN was introduced in optical communication systems. In [18], bi-directional RNNs have been successfully integrated to a short-range IM/DD fiber-optic system with sliding window sequence estimation. The bi-directional RNN outperforms the vanilla RNN by processing data in both directions, but it is not immune to the gradient vanishing problem, which makes its training rather intricate. Thereafter, the bi-directional gated recurrent unit (bi-GRU), equipped with gating mechanisms, can effectively address this issue and enhance the performance of bi-directional RNNs. The bi-GRU scheme has been successfully integrated into the E2E physical layer communication over AWGN channels [19], achieving considerable performance gains. However, it mainly focused on the E2E equalization at the receiver and its channel model was limited to AWGN and intersymbol interference channel. Moreover, a bi-GRU AE scheme was also introduced for prediction in a degradation system [20]. Those applications demonstrate the potential and effective of bi-GRU structures in optical communication systems where prediction and classification are required. Since E2E learned GCS fiber-optic system would process serial samples, system nonlinearities and receiver optimization, the bi-GRU structure can be integrated into the transceiver design.

In this paper, a bi-GRU enhanced E2E learning GCS structure is introduced in an optical WDM system to tackle the channel memory in auxiliary channel modeling and reach a system performance-complexity trade-off. First, we utilize bi-directional gated recurrent unit (bi-GRU), due to its decent performance and moderate complexity. The introduced cost-effective bi-GRU scheme could compensate for the potential learning setbacks for small stacks of FFNNs with respect to the combined influence of intersymbol interference and channel memory effects. Bi-directional long short-term memory (bi-LSTM) is utilized for performance and complexity comparison. Furthermore, in order to take channel memory effects into account, the FRP model is introduced for cost-effective and memory-aware optical channel modeling with linear and nonlinear coupled distortions [13], [21]. The combination of memory-aware cost-effective bi-GRU and FRP auxiliary channel can bring overall system GMI and MI gains with a trade-off in performance and complexity. Simulation results of learned GCS symbols in a 32 GBd 5-channel WDM 64QAM transmission over 800 km and 1280 km SSMF demonstrate that the proposed system can achieve better system performance in middle and long transmission distances than the benchmark FFNN-based scheme in terms of MI, GMI and Q-factor. Additionally, the proposed bi-GRU enhanced E2E learning requires lower computation complexity while providing similar system performance as the bi-LSTM.

The rest of this paper is organized as follows: Section II describes the proposed bi-GRU enhanced E2E learning scheme; Section III elaborates simulation system settings and model complexity evaluation; Section IV presents the results of the proposed scheme; and Section V concludes the paper.

II. Principles

A. Performance Metrics

In constellation shaping systems, these two criteria, MI and GMI, are commonly used to optimize the constellation and evaluate the trained results. MI is applied in symbol-wise systems while GMI is used in bit-wise systems, respectively. We assume $\boldsymbol{S}$ to be a complex constellation set with the cardinality $|\boldsymbol{S}| = M = 2^m$, where m denotes the bit number in one symbol. An m-dimensional binary vector random variable $\mathbf{X}$ is mapped into a complex symbol $X \in \boldsymbol{S}$ with a uniform probability mass function (PMF) $P_X(x) = 1/M$. In order to describe the impact induced by the channel, the channel transition probability is introduced as $p_{Y|X}(y|\ x)$, where X and $Y \in \mathbb{C}$ denote the complex value channel input and output, respectively. MI regarding the communication system represents the information shared by the channel input X and output Y, or the uncertainty of one random variable reduced by knowledge of another random variable. The definition of MI is expressed as follows [22]:

$$I(X;Y) = H(X) - H_p(X|Y), \tag{1}$$

where the entropy of random variable X and the conditional entropy of X given the variable Y are denoted as $H(X)$ and $H_p(X|Y)$, respectively. The expectation of the posterior probability is derived from the conditional entropy, indicating the correlation between the two random variables and the amount of shared information. Notably, the analytical calculation of the condition entropy is often intricate regarding optical communication systems. Therefore, approximations and simplified calculation methods are used during simulations, such as mismatched decoding [23], which refers to the suboptimal metrics used owing to the uncertainty of transition probability $p_{Y|X}(y|\ x)$. According to the principle of mismatched decoding, the approximated MI is calculated as

$$I(X;Y) \geq H(X) - \hat{H}_q(X|Y) = m - \hat{H}_q(X|Y). \tag{2}$$

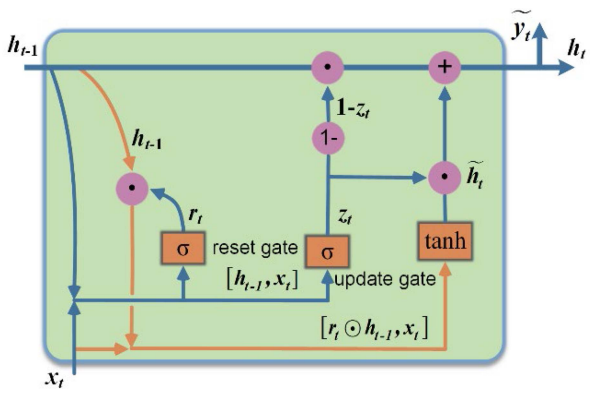

Fig. 1. Illustrative structure of a GRU memory unit.

$\hat{H}_q(X|Y)$ is formatted as an expectation $E[q_{X|Y}\ (x|\ y)]$, as the approximation of the analytical conditional entropy $H_p(X|Y)$. Therefore, the inequality occurs in (2) since the upper bound is used for practical calculation. When it comes to GMI, it is commonly used to evaluate the bit-wise systems such as bit-interleaved coded modulation (BICM). Thereafter, the symbol-wise forward error correction (FEC) for MI is replaced with binary FEC as for GMI. The estimated GMI is defined as follows:

$$I(\mathbf{X};Y) \geq H(x) - \sum_{i=1}^{m} \hat{H}_q(X_i|Y) = m - \sum_{i=1}^{m} \hat{H}_q(X_i|Y). \tag{3}$$

$\hat{H}_q(X_i|Y)$ is the conditional entropy formatted as $E\ [q_{X_i|Y}\ (x_i|\ y)]$ of the bit X_i at i-th position, given the channel output Y. The bit labeling is closely related to the estimation for the GMI. Gray labeling, commonly used in constellation shaping initialization, can reduce the gap between the GMI in (3) and its lower bound.

B. Bi-GRU Enhanced E2E Learning for M-QAM GCS

The GRU unit reduces its complexity by simplifying three gate mechanisms in a LSTM unit into a reset gate and an update gate, while achieving similar performance. The final output of the GRU unit is calculated by both current input x_t and previous state h_{t-1} with the collective effect of these gates. The outputs of the internal gates for the GRU unit are summarized as follows:

$$\begin{aligned} r_t &= \sigma(W_r \cdot [h_{t-1}, x_t] + b_r), \\ z_t &= \sigma(W_z \cdot [h_{t-1}, x_t] + b_z), \\ \widetilde{h}_t &= \tanh(W_h \cdot [r_t \odot h_{t-1}, x_t] + b_h), \\ h_t &= (1 - z_t) \odot h_{t-1} + z_t \odot \widetilde{h}_t, \end{aligned} \tag{4}$$

where W_r, W_z and W_h are the weight matrices for reset gate, update gate and new memory calculation, respectively. b_r, b_z, b_h are corresponding bias vectors. σ is the sigmoid function for reset and update gate. In new memory calculation, *tanh* is the hyperbolic tangent activation function, and $\odot$ represents the Hadamard product. Fig. 1 presents the internal structure of a basic GRU cell [16]. The memory-awareness is expressed by the transceiver end-to-end scheme design. Bi-GRU is utilized to replace the FFNN-based end-to-end scheme to learn the intersymbol interference using its bi-directional sample feature extraction ability.

A basic E2E learning scheme mainly consists of two NNs, an encoder NN and a decoder NN, respectively. The input one-hot vectors of constellation size M are mapped by the encoder NN to symbols in the complex plane through nonlinear transformations. Estimates of posterior probabilities of the encoded vectors are calculated at the decoder NN. The bi-directional structure is composed of two stacked unidirectional units in forward and backward directions, respectively [24]. The bi-directional structure can capture patterns from adjacent data at each timeslot. The channel embedded between the transceiver NNs during training is a differentiable channel model.

At the transmitter, the one-hot encoded vector is denoted as $\boldsymbol{s}_t \in \{\boldsymbol{e}_i | i = 1, 2, \ldots, M\}$ for symbol-wise encoder input, where $\boldsymbol{e}_i$ is the one-hot coding with all zero elements but a one at position i. For bit-wise scenario, the input block of m bits $\boldsymbol{s}_t$, rather than one-hot encoded vector, is selected from a set of all possible m-bit sequences $\{0, 1\}^m$. Thereafter, current symbol at the t-th timeslot $\boldsymbol{s}_t$ $(t = 1, 2, \ldots, T)$ with its k neighboring symbols in both directions are concatenated as $\boldsymbol{x}^{(t)} = [\boldsymbol{s}_{t-k}, \ldots, \boldsymbol{s}_t, \ldots, \boldsymbol{s}_{t+k}]$ to serve as one input sequence batch for the bi-GRU network. In the bi-GRU network layer, the length of input sequence $2k + 1$ determines recurrent time steps of the bi-GRU model and further impacts the overall E2E learning performance. We note that a long sequence input will be time-consuming for bi-GRU training, while it doesn't achieve better performance.

The encoder bi-GRU hidden states $\boldsymbol{h}_t$ are calculated through all the recurrent timesteps and the output of the bi-GRU model layer are fully connected to the linear layer for complex symbol transmission in the optical auxiliary channel. In terms of AE GCS, the encoder is trained to learn the constellation and the decoder captures the pattern for the decision boundaries with a learned constellation and the corresponding channel model. In our proposed scheme, the encoder enhanced by bi-GRU is capable to learn not only the constellation for one symbol sample or one block of bits, but also the interference of adjacent samples.

To realize a cost-effective and memory-aware channel modeling, the FRP auxiliary channel, is utilized for the constellation training with variable branch sizes for different fiber span lengths. Details of the FRP model will be elaborated later. The performance of the learned constellation is evaluated using the computation-demanding but precise SSFM. To ensure the structure of AE, the basic receiver DSP blocks are included in channel components. Specifically, the root-raised cosine filter, chromatic dispersion compensation (CDC), and carrier phase estimation (CPE) blocks are utilized in the DSP chain.

The transmitted complex signal sequence of length $2k + 1$ serves as the decoder bi-GRU input, resulting a posterior probability vector $\boldsymbol{r}_t$. Using a softmax output layer in the symbol-wise case, the sum of $\boldsymbol{r}_t$ for all the M categories equals to 1, indicating the choice of a categorical cross-entropy (CE) for the cost function in terms of MI. After the iteration of a training set, the trainable AE weights are optimized and the categorical CE loss function is minimized. Considering one iteration, the

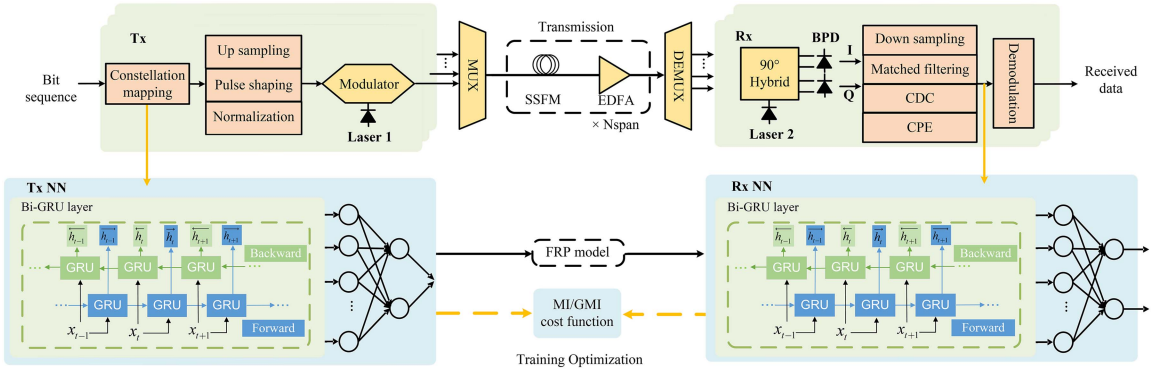

Fig. 2. Structure of the bi-GRU E2E GCS learning scheme, trained over FRP model and validated over SSFM.

whole training set is departed into batches with a size B and the categorical CE loss function is denoted as [22], where i denotes the i-th element of the output vector.

$$L_{CE}(\boldsymbol{w}) = \frac{1}{B}\sum_{t=1}^{B}\left[-\sum_{i=1}^{M} s_t^i \log r_t^i\right]. \tag{5}$$

When it comes to the bit-wise case, $\boldsymbol{r}_t$ refers to bit-level posterior probability, where softmax activation function is replaced with the sigmoid function. Here i denotes the i-th element of the m-dimensional output. Since this is a binary classification, the loss function binary cross-entropy (BCE) is defined as [22]:

$$L_{BCE}(\boldsymbol{w}) = \frac{1}{B}\sum_{t=1}^{B}\left[-\frac{1}{m}\sum_{i=1}^{m} s_t^i \log r_t^i + (1-s_t^i)\log(1-r_t^i)\right]. \tag{6}$$

During the training, we optimize the geometric shaped constellations in terms of CE and BCE via a batch gradient descent procedure, i.e., by a repeated generation of the training symbols' batches of fixed size and updating the trainable parameters. In both cases, CE and BCE represent the approximation conditional entropy in (2) and (3), respectively. Therefore, minimizing the loss function implies maximizing the MI and GMI metrics.

Given the performance metrics of MI and GMI, GCS aims at the position optimization of the constellation points by maximizing these metrics. As depicted in Fig. 2, the schematic plot of the proposed AE structure for E2E GCS is presented with the bi-GRU enhanced transceiver blocks and a memory-aware auxiliary channel FRP. Similar to conventional FFNN-based AE GCS, here the encoder and decoder are also modeled as parametric functions with a set of trainable weights $\boldsymbol{w} = \{\boldsymbol{w}_{enc}, \boldsymbol{w}_{dec}\}$. Those weights are trained and optimized to lower the cost function formatted with the input and output of the E2E learning scheme. Considering the different formats of those performance metrics, the cost function is determined by either categorical CE for MI (symbol-wise) or BCE for GMI (bit-wise).

C. The Auxiliary Channel Model FRP

The Manakov equation is commonly applied to model the propagation of the dual-polarization optical signal in a fiber-optic channel with lumped amplifiers, such as erbium-doped fiber amplifier (EDFA) [25]. The Manakov equation is expressed as:

$$\begin{aligned}\frac{\partial \mathbf{u}}{\partial z} &= i\frac{8}{9}\gamma f(z)\|\mathbf{u}\|^2\mathbf{u} - i\frac{\beta_2}{2}\frac{\partial^2 \mathbf{u}}{\partial t^2} + \eta(z,t)\\ f(z) &= \exp(-\alpha(z - L_{sp}\lfloor z/L_{sp}\rfloor)),\end{aligned} \tag{7}$$

where $\mathbf{u}$ is the complex envelop of the optical field, z denotes the transmission distance, and t is the time. Here $f(z)$ models the optical loss and amplification accumulated at z, with α as the attenuation, L_{sp} is the fiber span length, β_2 and γ is the group velocity dispersion and nonlinear coefficient, respectively; $\eta(z,t)$ denotes the amplified spontaneous emission (ASE) noise induced by optical amplifiers (OAs). Stepwise dispersion and nonlinear operators are alternatively calculated in numerical simulation, namely SSFM [26]. The step size of the SSFM simulation can be reduced for more precision.

In E2E learning with gradient backpropagation, a cascade of convolutional NN layer stacks is used to replace the conventional SSFM. However, the calculation complexity of such layers leads to numerical error accumulation, causing computational instability such as gradient vanishing or explosion [27]. Therefore, a simplified differentiable auxiliary channel model is imperative under conditions of E2E learning. Auxiliary channel model can reduce the numerical complexity of E2E learning to a large extent by sacrificing the precision of channel approximation with smaller shaping gains, providing a trade-off between performance and complexity.

In our proposed scheme, FRP channel model is utilized to enhance the memory-awareness. Combined with the intersymbol interference feature extraction provided by bi-GRU memory units, the FRP-based end-to-end learning scheme could further express and exploit the channel memory information. The FRP model can be regarded as a simplified SSFM model with a weakly nonlinear regime approximation [13], [21]. Specifically, the FRP model is the first order approximation of SSFM regarding the nonlinear parameter γ, indicating that it ignores the effect of all the nonlinear steps on each other and simplifies the exponent term in the nonlinear step of SSFM to a linear approximation. The channel output [13], taking account of the

perturbation from the signal $\mathbf{u}$, is expressed as:

$$\begin{aligned}\mathbf{u}(z,t) &= \mathbf{u}_L(z,t) + \mathbf{u}_{NL}(z,t) + O(\gamma^2),\\ \mathbf{u}_L(z,t) &= D_z[\mathbf{u}(0,t) + \eta(z,t)],\\ \mathbf{u}_{NL}(z,t) &= \sum\nolimits_{m=1}^{n_{st}} D_{z-(m\delta)}[N_{\delta,m}[\mathbf{u}_L(m\delta,t)]],\end{aligned} \tag{8}$$

and

$$\begin{aligned}D_z[\centerdot] &= \mathbb{F}^{-1}[\exp(i\beta_2 z\omega^2/2)\mathbb{F}[\centerdot]],\\ N_{\delta,m}[\mathbf{u}(t)] &= i\frac{8}{9}\gamma L_{eff} f(m\delta)\|\mathbf{u}(t)\|^2\mathbf{u}(t), \delta = \frac{z}{n_{st}}\\ L_{eff} &= \frac{1-e^{-\alpha\delta}}{\alpha}.\end{aligned}$$

Here n_{st} is the calculation steps in nonlinear section $\mathbf{u}_{NL}$, and δ is the corresponding step size in distance. $\mathbb{F}$ and $\mathbb{F}^{-1}$ is the Fourier transform (FT) and inverse FT, respectively, and $\|\cdot\|$ is the Euclidean norm. D_z is the accumulated chromatic dispersion operator at link length z, while $N_{\delta,m}$ denotes the combined effect of nonlinearity and attenuation accumulated over length δ, centered around the point $m\delta$. L_{eff} is effective step length. According to (8), the linear and nonlinear terms can be calculated in a parallel fashion. Therefore, the total calculation step $n_{st}+1$ for the simulated link length z determines the precision of approximation and complexity in FRP. All the noises accumulated throughout the total link length are added in $u_L(z,\ t)$, while the ASE noise with weighted power spectral density scaled to $m\delta$ is injected into each calculation step in all the nonlinear terms [13].

III. Simulation Setup and Complexity Analysis

A. Numerical Simulation Setup

Numerical simulation of the optical coherent WDM system is implemented with five optical transmitters ($Tx1$, …, $Tx5$) spaced by 50 GHz, each of which transmitting 32 GBd signals. As is depicted in Fig. 2, the optimal constellations are optimized by the joint of bi-GRU and FRP scheme with MI or GMI performance metric. With the oversampling factor 16 samples/symbol, the transmitted samples are pulse shaped by the root-raised cosine filter with a 0.02 roll-off factor. The resulting signal in each channel is normalized to input power for optical transmission. These signals are added together in the multiplexer to form a WDM signal. This WDM signal is transmitted over an optical fiber channel modeled by SSFM, which simulates a link of N_{span} EDFA-amplified spans of 80km SSMF. At the receiver, the demultiplexed signal is processed by the coherent detection. The central channel is filtered out by a low pass filter, which in this case is the root-raised cosine matched filter. CDC is performed in frequency domain and CPE is utilized to compensate the accumulated phase rotation. The received data are processed with DSP before the calculation of Q-factor, defined as $\mathrm{Q} = 20\lg[\sqrt{2}erfc^{-1}(2BER)]$ for performance evaluation [28]. Some key parameters of system overall layout and optical fiber channel used in the simulations are listed in Table I.

The structures of bi-GRU and bi-LSTM are built, trained and evaluated in Tensorflow 1.14.0. The SSFM and FRP model are developed in python version to accommodate the bi-GRU, bi-LSTM and FFNN structures. In our model, Adam optimizer is employed for optimization. The whole data set is divided into training (70%) and validation (30%). The time sliding window $2k+1$ is set to 21 for the capture of adequate serial information in bi-GRU-based schemes. The number of maximum training epochs is set to 300. The learning rate is set to 0.002. The early stopping scheme is also implemented when the accuracy does not improve for 25 successive epochs to prevent overfitting. The linear hidden layer nodes are set to 128, and FFNN consists of 3 hidden layers as the baseline, while there is only two linear layers in bi-GRU and bi-LSTM scenarios. The number of units for bi-GRU and bi-LSTM cells are set to 128. Those neural network hyperparameters are set so as to achieve a complexity-performance balance. It is noted that with the increase of the layers and nodes, the computational expense would increase without considerable performance improvement. Other parameters for FFNN and bi-GRU-based scheme are the same for comparison. All the simulations were conducted on a personal computer with Intel Core i5-9400F CPU @ 2.90 GHz, 16 GB Random Access Memory (RAM), and GeForce 1050Ti GPU. Due to the limitation of our computation equipment, the computational time was relatively long, but we conducted the simulation on this specific computer. Therefore, all the results are obtained with the same computational baseline.

TABLE I
Parameters of the Transmission Link

Parameters	Value
Carrier wavelength	1550 nm
Symbol rate	32 GBd
Attenuation	0.2 dB/km
Dispersion	16.464 ps/(nm·km)
Nonlinear coefficient	1.3 W^{-1}/km
Span length	80 km
Noise figure	5 dB

B. Complexity Analysis

The complexity of the proposed bi-GRU enhanced E2E learning structure is compared with bi-LSTM-based model. The number of parameters in both bi-GRU and bi-LSTM layers are considered analytically. The complexity comparison of bi-GRU, bi-LSTM with FRP channel model and FFNN-based SSFM channel model for E2E GCS learning will be presented from the perspective of running time in Section IV.

In the bi-GRU model, the GRU cell is the main component with two gates and cell state [16]. The input of current GRU cell is denoted as $x_t \in \mathrm{R}^{1\times \mathrm{d\_in}}$, and the output of the previous cell is $h_{t-1} \in \mathrm{R}^{1\times \mathrm{d\_hid}}$. Due to the symmetry of the GRU equations, we firstly focus on the weight matrix in reset gate for concatenated input x_t and previous state h_{t-1},which is

$W_r \in \mathrm{R}^{(\mathrm{d\_in}+\mathrm{d\_hid})\times \mathrm{d\_hid}}$. The bias vector is $b_r \in \mathrm{R}^{1\times \mathrm{d\_hid}}$. Since there are weight and bias variables for two gates and one cell state, the number of parameters in one GRU unit can be summed as:

$$N_{GRU\_P} = 3 \times [(d_{in} + d_{hid})d_{hid} + d_{hid}]. \tag{9}$$

The bi-GRU layer is stacked by two GRUs, thereafter, the number of parameters of bi-GRU layer is $2\times N_{GRU\_P}$. Since the dimension of the bi-GRU layer output is $1 \times 2d_{hid}$, the number of parameters contributed by the cascaded Dense layer is $2d_{hid}\times d_{out}$ for weight and $1 \times d_{out}$ for bias, where d_{out} is the final output dimension. Due to the identical network structure of the bi-GRU-based encoder and decoder, the parameter number of the bi-GRU encoder/ decoder can be summarized as:

$$N_{biGRU\_P} = 2 \times 3[(d_{in} + d_{hid} + 1)d_{hid}] + (2d_{hid} + 1)d_{out}. \tag{10}$$

For each LSTM unit [17], parameters of an LSTM unit contain weight matrices and bias for three gates and one cell state. Therefore, given the same parameter settings, the LSTM entails a 25% of parameter extra usage. Deduced by analogy, the number of parameters of the bi-LSTM encoder/ decoder can be calculated as follows:

$$N_{biLSTM\_P} = 2 \times 4[(d_{in}+d_{hid}+1)d_{hid}] + (2d_{hid} + 1)d_{out}. \tag{11}$$

From those aforementioned equations, it can be seen that under the identical input feature and hidden unit settings of the network, bi-GRU has fewer parameters than bi-LSTM. Moreover, the running time of the three scenarios will be demonstrated in the next section.

IV. Results and Discussion

A. Performance of the FRP Model

Although the FRP model utilizes a simplified first-order perturbation in fiber nonlinearity, it offers a close approximation of the SSFM model. We consider the performance of FRP and SSFM when modelling the propagation of square 64QAM signal after the 960 km 5-channel WDM optical coherent system with ASE noise. Here we note the proper setting of step size defined by the total calculation step in the FRP model will impact the performance. The calculation steps comprise 345 steps in nonlinear terms and 1 step in linear term in the FRP, resulting a step size of 3.468 km. The step size dz is set to 0.2 km for the SSFM.

In Fig. 3(a), the effective signal-to-noise ratio (SNR) curves of the received signals after CDC and CPE are depicted. The proximity of SNR under both models is observed in the weakly nonlinear regime from -6 to -2 dBm in launched optical power (LOP), and the matching of the two models is still acceptable near the optimal LOP at -1 dBm. However, the performance of the FRP model is deviated due to its limited approximation ability in the high nonlinear regime, when the LOP exceeds 2 dBm. We can further observe matching curves of MI and GMI performance in Fig. 3(b) and (c), indicating that the FRP model achieves a similar system performance with a larger step size compared with the SSFM. Moreover, the calculation of the

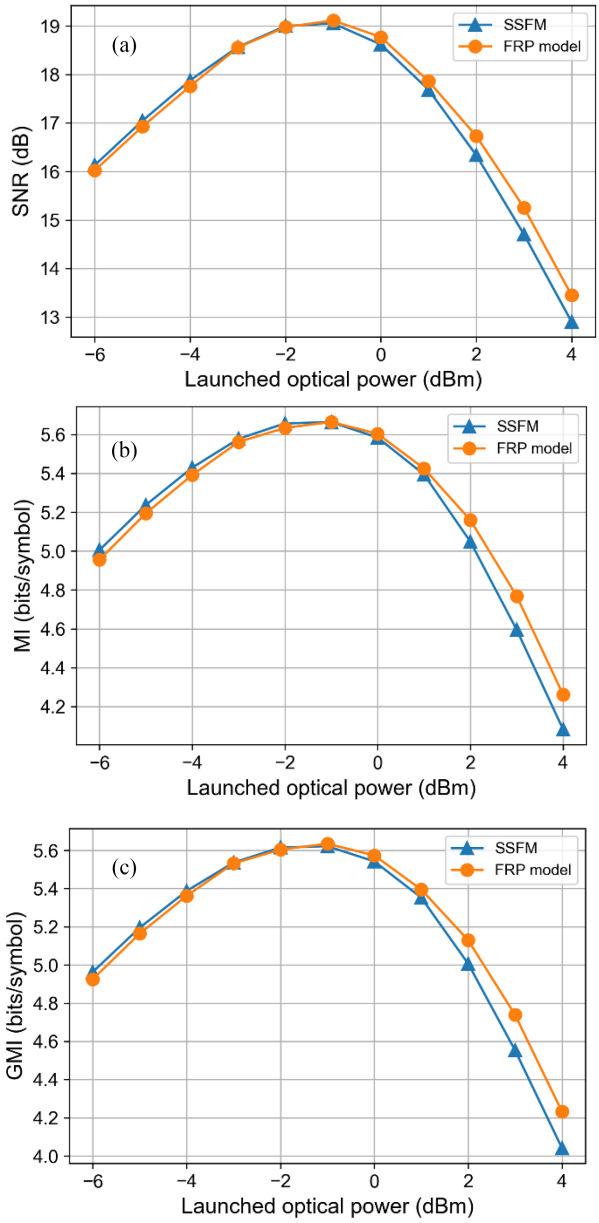

Fig. 3. Comparison between channel models based on first-order regular perturbation (FRP) and split-step Fourier method (SSFM) transmitting square 64QAM in (a) SNR, (b) MI, and (c) GMI.

FRP is feasible and efficient for gradient propagation since the complicated higher-order fiber nonlinearity is omitted. Owing to its parallel calculation feature, the FRP model completes the LOP sweep in 8 min 18 s, reducing ∼80% of the simulation running time compared with 40 min 15 s for the serial SSFM with the same computing resources.

Fig. 4 demonstrates the FFNN-based E2E GCS 64QAM constellations trained and optimized with MI and GMI respectively at optimal LOP from the two models in the above WDM optical coherent system after 960 km. The optimization of the four constellations in Fig. 4 has been conducted under such system settings after a training epoch of 300, when convergence has been observed in our simulation platform. The optimal

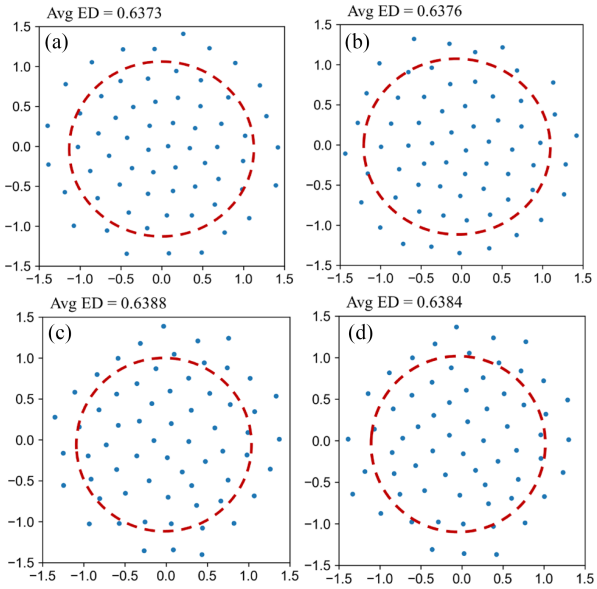

Fig. 4. Constellations of shaped 64QAM using MI optimized (a) FRP and (b) SSFM channel model, compared with GMI optimized (c) FRP and (d) SSFM channel model for 960 km @ optimal LOPs.

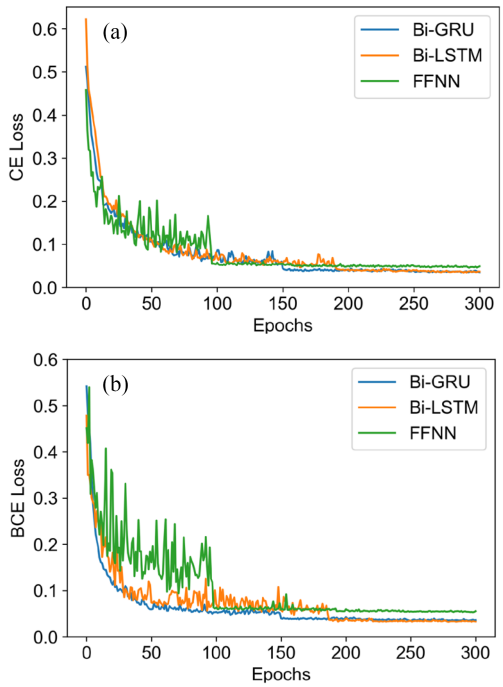

Fig. 5. Training convergence of (a) CE and (b) BCE loss optimized for different E2E GCS schemes in FRP channel.

constellations are chosen under the repeated simulations of a fixed training epochs after convergence is reached. We select the constellation with the minimum loss in both MI and GMI optimized procedure after convergence. The Euclidean distance is a common distance metric used to calculate the distance between two points in multi-dimensional space. The average Euclidean distance (AED) is defined as taking the average of the Euclidean distances calculated between multiple vectors. This type of metric is widely used in clustering analysis and classification problems [29].

Here we vectorize the constellation points and compare the two AEDs in the circled area. For MI and GMI optimization, with relatively low energies for symbols in the red circles, similar AEDs around 0.637 and 0.638 for both channel models are observed. Thereafter, the FRP model offers a relatively good approximation for the precise SSFM model in the weakly nonlinear regime and around the optimal LOP level, which corresponds to the results in Fig. 3. Symbols at peripheral areas are prone to fiber nonlinear impairments. The minimum Euclidean distance (MED), a commonly-used performance metric between symbols in the constellation, is utilized [30]. The bit error rate (BER) and effective SNR performance in the optical communication system are inversely dependent on the MED. In terms of MI, given the identical symbol average power, the MED of symbols with higher energy (those outside the red circle) for the FRP and SSFM model is 0.3495 and 0.3342, respectively. Regarding GMI optimization, the MED of peripheral symbols is 0.3186 and 0.3157, respectively. Both optimization metrics show similar MED trends. Namely, a larger MED value of the FRP learned constellation would cause the difference in SNR performance in higher LOP region. Therefore, it is noted that when higher LOP is required, FRP model deviates from the SSFM to a certain extent due to the lack of approximation ability in high order nonlinearity. In this study, the long-haul WDM transmission scheme requires a relatively low LOP to achieve adequate transmission performance.

Thereafter, the FRP model can provide acceptable approximation to the SSFM in performance, while taking less running time in simulation, serving as a cost-effective yet valid training model for E2E GCS learning.

The corresponding training convergence of three different neural network schemes optimized with CE and BCE loss are shown in Fig. 5. Similar convergence trends are observed in Fig. 5(a) and (b) with a faster convergence speed for the FFNN due to its simpler network structure compared with bi-GRU and bi-LSTM. However, both bi-GRU and bi-LSTM could converge to a lower loss value than that of the FFNN, producing better optimized constellations. It is also observed that the convergence speed of the bi-GRU around 150 epochs is relatively faster than the bi-LSTM, due to simplified memory cell units in the bi-GRU architecture. Therefore, as for the bi-GRU scheme, the convergence speed and the minimization of both loss functions have reached a trade-off in computational complexity and performance.

B. Performance of Bi-GRU Enhanced E2E GCS Learning

To assess the performance of the proposed scheme, referred to bi-GRU enhanced GCS, we compare it to the conventional square QAM, to an optimized FFNN-based E2E learning scheme, and to the bi-LSTM-based scheme. For a fair comparison, the architectures of all the schemes and baseline are identical and the FFNN-based scheme is optimized through adequate training and learning. Fig. 6 shows the results of the numerical simulation after 800 km 5-channel

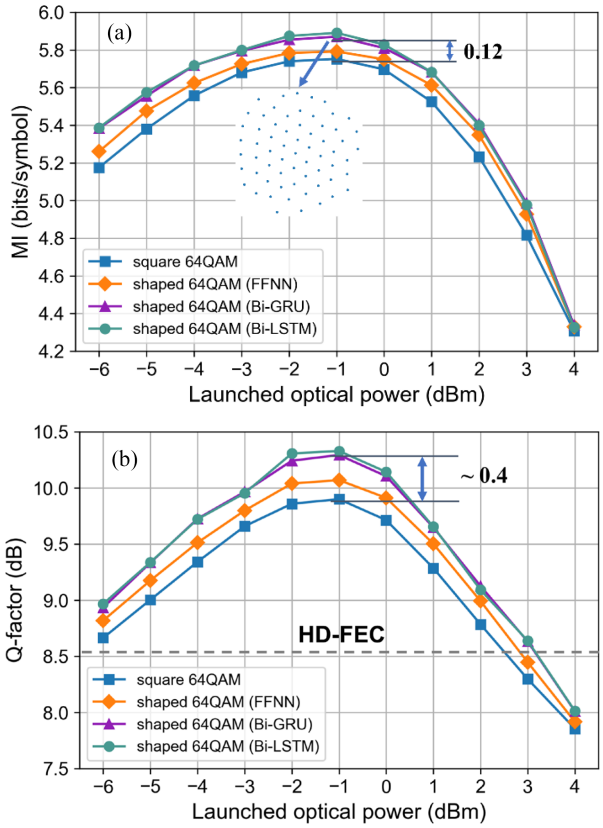

Fig. 6. Performance comparison of different E2E GCS schemes at 800 km in (a) MI and (b) Q-factor.

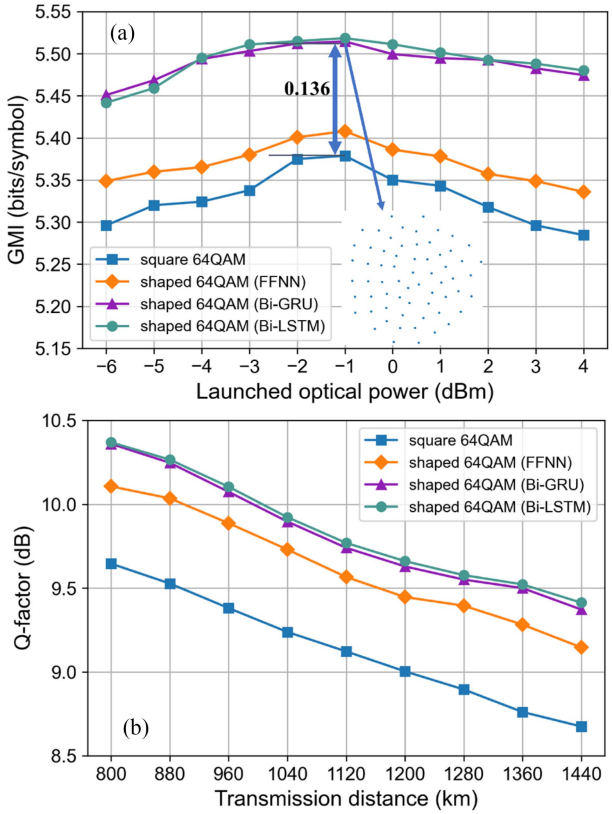

Fig. 7. Performance comparison of E2E GCS schemes in (a) GMI at 1280 km and (b) Q-factor under different transmission distances @ optimal LOP.

WDM optical coherent transmission under the range of LOP from −6 to 4 dBm. It is noted that the training process is carried out at the optimal LOP for better constellation shaping performance.

It can be seen that there is an overall performance improvement for FFNN-based and bi-GRU enhanced shaping compared to the unshaped QAM constellations in both MI and Q-factor, which is calculated from the BER. Compared to square 64QAM, the MI could reach a gain of 0.12 bits/symbol at the optimal LOP for the bi-GRU enhanced shaping at 5.87 bits/symbol in Fig. 6(a). Similarly, Fig. 6(b) indicates that there is a performance improvement in terms of the Q-factor compared to square 64QAM at their optimal LOP. The bi-GRU enhanced learning outperforms square 64QAM by about 0.4 dB in Q-factor. With the aid of receiver DSP, the Q-factors in all scenarios exceed the HD-FEC limit of 8.52 dB around the optimal LOP region. The performance of the bi-GRU and bi-LSTM-based learning is nearly identical, with some neglectable fluctuations in both performance metrics.

Fig. 7(a) shows the results of the numerical simulation after 1280 km 5-channel WDM optical coherent transmission at LOP ranging from −6 to 4 dBm. Based on the bit-wise training procedure with the loss function of BCE, the optimal LOP is selected to validate the results. It can be seen that there is an overall performance improvement for FFNN-based and bi-GRU enhanced shaping compared to the square 64 QAM constellations in GMI. It is noted that the results of the bi-LSTM-based learning scheme is similar to the trends in Fig. 6, indicating neglectable GCS performance difference between the two flavors of bi-directional recurrent networks. Compared to square 64 QAM, the system GMI at 1280 km could reach a gain of 0.136 bits/symbol at optimal LOP -1 dBm for the bi-GRU enhanced shaping at 5.5146 bits/symbol in Fig. 7(a).

Furthermore, the bi-GRU enhanced performance gain in GMI compared to FFNN-based E2E learning is 0.1065 bits/symbol, indicating the effective GMI gain aided by the bi-GRU scheme. The performance of bi-LSTM is similar to that of the bi-GRU, as indicated in Fig. 6. Fig. 7(b) demonstrates the Q-factor at optimal LOP in different distances. Compared to square 64 QAM at the optimal LOP, the bi-GRU enhanced learning outperforms square 64 QAM by about 0.65 dB in Q-factor at 1280 km. There is also an improvement in Q-factor compared to FFNN-based GCS 64 QAM of about 0.2 dB. Moreover, given the same Q-factor at 9.3 dB, the transmission distance for bi-GRU enhanced FRP model is extended by 160 km compared to FFNN-based GCS scheme. This indicates better nonlinearity tolerance for the proposed scheme since there is a larger Q-factor gain at a longer distance.

Fig. 8 presents a training time comparison of 64 QAM 5-channel WDM optical coherent system E2E GCS learning with FFNN-based SSFM channel model (step size set as 0.1 km), bi-LSTM and bi-GRU-based FRP model. Only the training time of MI optimized system (800 km) is depicted because the GMI

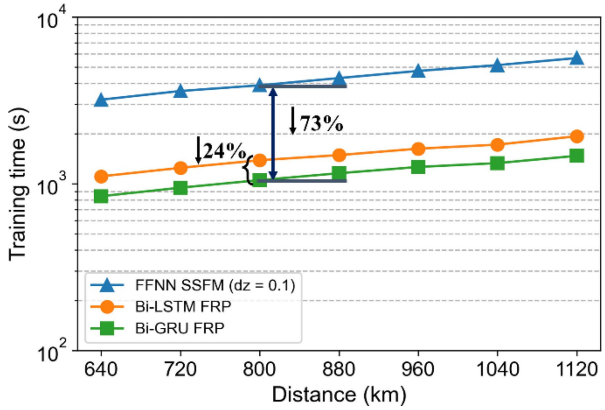

Fig. 8. Training time vs. distances for SSFM, bi-LSTM and bi-GRU E2E learning scheme.

optimized training time shows similar trends. It is noticeable that the GCS symbols are trained and trainable variables are saved before the validation in optical fiber channel.

The training time, averaged after multiple simulations, refers to the complete E2E GCS training expense, while the validations are carried out on the same SSFM channel, which is excluded from the training time. The training time under different distance of the learning process is recorded under the same hardware and software simulation conditions as listed above. It is noted that there is a linear increase trend in the training time with the transmission distance for both FRP and SSFM models. Moreover, as the complexity derived in Section III, fewer parameters lead to shorter running time and less computational overhead.

Based on previous simulation results, the Q-factor performances of bi-GRU and bi-LSTM AE GCS schemes are similar, while the number of parameters of bi-GRU E2E learning scheme is 25% less than that of bi-LSTM, resulting the shorter average training time. From Fig. 8, when the transmission distance is 800 km, the bi-GRU-based FRP training time (1051 s) reduces about 73% of that for the FFNN-based SSFM (3895 s) and it also reduces about 24% of training time than the bi-LSTM (1384 s). Therefore, with similar performance, the bi-GRU scheme has lower computational cost than that of the bi-LSTM. Given the effective performance of FRP near optimal LOP, the proposed scheme cost than that of the bi-LSTM. The training expense reduction of 24% here in schematic design will greatly impact the higher-order constellation training process since it requires a larger neural network to realize convergence. Therefore, a model like bi-GRU that trains faster than bi-LSTM can be more cost-effective, especially in large-scale applications or when computational resources are limited.

V. Conclusion

In this paper, a bi-GRU enhanced E2E learning for GCS in WDM optical coherent communication system is proposed. The performance of bi-GRU has been verified and compared to FFNN and bi-LSTM through a 32 GBd 5-channel WDM 64 QAM 800 km and 1280 km optical coherent communication system in terms of MI and GMI, respectively. The FRP model is introduced to facilitate the bi-GRU encoder and decoder scheme for capturing features and learning the interference in neighboring sequential symbols. Validation of the FRP has been demonstrated in the comparison with SSFM model, and acceptable matching of SNR and MI at LOP could be observed. The complexity of bi-GRU and bi-LSTM are theoretically analyzed. Simulations show that the bi-GRU produces both Q-factor and MI improvements of 0.4 dB and 0.12 bits/symbol respectively compared to conventional square 64 QAM schemes. Bi-GRU provides a similar performance to bi-LSTM with less computation resources. At 1280 km, compared with square 64 QAM in terms of GMI and Q-factor, an improvement of 0.136 bits/symbol and 0.65 dB has been observed. Owing to its learning capability for inter-symbol effect, the bi-GRU enhanced scheme trained with multiple symbols has further obtained gains over the FFNN-based structure. Although bi-GRU takes more multiplications than basic FFNN, it offers better performance in system capacity and signal transmission quality. While the overall complexity of the proposed bi-GRU enhanced E2E learning is relatively high compared to a simple FFNN and AWGN-based scheme, a more accurate description of the optical channel can be provided, and considerable improvements can be achieved by the proposed scheme. Those results indicate that bi-GRU is a promising alternative for E2E GCS scenario in performance and complexity trade-off, and it has the potential to further push the boundary of spectral efficiency in long-haul GCS E2E learning WDM systems.

References

[1] T. Fehenberger, A. Alvarado, G. Bocherer, and N. Hanik, "On probabilistic shaping of quadrature amplitude modulation for the nonlinear fiber channel," *J. Lightw. Technol.*, vol. 34, no. 21, pp. 5063–5073, Nov. 2016, doi: 10.1109/JLT.2016.2594271.

[2] D. S. Millar, T. Fehenberger, T. Koike-Akino, K. Kojima, and K. Parsons, "Distribution matching for high spectral efficiency optical communication with multiset partitions," *J. Lightw. Technol.*, vol. 37, no. 2, pp. 517–523, Jan. 2019, doi: 10.1109/JLT.2018.2887188.

[3] T. O'Shea and J. Hoydis, "An introduction to deep learning for the physical layer," *IEEE Trans. Cogn. Commun. Netw.*, vol. 3, no. 4, pp. 563–575, Dec. 2017, doi: 10.1109/TCCN.2017.2758370.

[4] B. Karanov et al., "End-to-end deep learning of optical fiber communications," *J. Lightw. Technol.*, vol. 36, no. 20, pp. 4843–4855, Oct. 2018, doi: 10.1109/JLT.2018.2865109.

[5] S. Li, C. Häger, N. Garcia, and H. Wymeersch, "Achievable information rates for nonlinear fiber communication via end-to-end autoencoder learning," in *Proc. IEEE Eur. Conf. Opt. Commun.*, 2018, pp. 1–3.

[6] R. T. Jones et al., "Geometric constellation shaping for fiber optic communication systems via end-to-end learning," 2018, *arXiv:1810.00774*.

[7] R. T. Jones, T. A. Eriksson, M. P. Yankov, and D. Zibar, "Deep learning of geometric constellation shaping including fiber nonlinearities," in *Proc. IEEE Eur. Conf. Opt. Commun.*, 2018, pp. 1–3.

[8] R. T. Jones, M. P. Yankov, and Z. Darko, "End-to-end learning for GMI optimized geometric constellation shape," in *Proc. IEEE Eur. Conf. Opt. Commun.*, 2019, pp. 1–3.

[9] K. Gümüs, A. Alvarado, B. Chen, C. Häger, and E. Agrell, "End-to-end learning of geometrical shaping maximizing generalized mutual information," in *Proc. IEEE Opt. Fiber Commun. Conf. Exhib.*, 2020, pp. 1–3.

[10] T. Uhlemann, S. Cammerer, A. Span, S. Dörner, and S. Brink, "Deep-learning autoencoder for coherent and nonlinear optical communication," in *Proc. IEEE 21st ITG-Symp.*, 2020, pp. 1–8.

[11] P. Poggiolini, "The GN model of non-linear propagation in uncompensated coherent optical systems," *J. Lightw. Technol.*, vol. 30, no. 24, pp. 3857–3879, Dec. 2012, doi: 10.1109/JLT.2012.2217729.

[12] R. Dar, M. Feder, A. Mecozzi, and M. Shtaif, "Properties of nonlinear noise in long, dispersion-uncompensated fiber links," *Opt. Exp.*, vol. 21, no. 22, pp. 25685–25699, Oct. 2013, doi: 10.1364/OE.21.025685.

[13] V. Neskorniuk et al., "End-to-end deep learning of long-haul coherent optical fiber communications via regular perturbation model," in *Proc. IEEE Eur. Conf. Opt. Commun.*, 2021, pp. 1–4.
[14] I. Goodfellow, Y. Bengio, and A. Courville, "Sequence modeling: Recurrent and recursive nets," in *Deep Learning*, Cambridge, MA, USA: MIT Press, 2016, ch. 10, pp. 363–408.
[15] K. Greff, R. K. Srivastava, J. Koutník, B. R. Steunebrink, and J. Schmidhuber, "LSTM: A search space odyssey," *IEEE Trans. Neural Netw. Learn. Syst.*, vol. 28, no. 10, pp. 2222–2232, Oct. 2017, doi: 10.1109/TNNLS.2016.2582924.
[16] K. Cho et al., "Learning phrase representations using RNN encoder-decoder for statistical machine translation," in *Proc. Conf. Empirical Methods Natural Lang. Process.*, 2014, pp. 1724–1734.
[17] S. Deligiannidis, C. Mesaritakis, and A. Bogris, "Performance and complexity evaluation of recurrent neural network models for fibre nonlinear equalization in digital coherent systems," in *Proc. IEEE Eur. Conf. Opt. Commun.*, 2020, pp. 1–4.
[18] B. Karanov, D. Lavery, P. Bayvel, and L. Schmalen, "End-to-end optimized transmission over dispersive intensity-modulated channels using bidirectional recurrent neural networks," *Opt. Exp.*, vol. 27, no. 14, pp. 19650–19663, Jun. 2019, doi: 10.1364/OE.27.019650.
[19] H. Wu, Y. Zhang, X. Zhao, N. Zhu, and M. Coates, "End-to-end physical layer communication using bi-directional GRUs for ISI channels," in *Proc. IEEE Globecom Workshops*, 2020, pp. 1–6.
[20] Y. Duan, H. Li, M. He, and D. Zhao, "A BiGRU autoencoder remaining useful life prediction scheme with attention mechanism and skip connection," *IEEE Sensors J.*, vol. 21, no. 9, pp. 10905–10914, May 2021, doi: 10.1109/JSEN.2021.3060395.
[21] A. Vannucci, P. Serena, and A. Bononi, "The RP method: A new tool for the iterative solution of the nonlinear Schrodinger equation," *J. Lightw. Technol.*, vol. 20, no. 7, pp. 1102–1112, Jul. 2002, doi: 10.1109/JLT.2002.800376.
[22] O. Jovanovic, F. Da Ros, D. Zibar, and M. P. Yankov, "Geometric constellation shaping for fiber-optic channels via end-to-end learning," *J. Lightw. Technol.*, vol. 41, no. 12, pp. 3726–3736, Jun. 2023, doi: 10.1109/JLT.2023.3276300.
[23] D. M. Arnold, H. Loeliger, P. O. Vontobel, A. Kavcic, and W. Zeng, "Simulation-based computation of information rates for channels with memory," *IEEE Trans. Inf. Theory*, vol. 52, no. 8, pp. 3498–3508, Aug. 2006, doi: 10.1109/TIT.2006.878110.
[24] C. Xiong, S. Merity, and R. Socher, "Dynamic memory networks for visual and textual question answering," in *Proc. 33rd Int. Conf. Int. Conf. Mach. Learn.*, 2016, pp. 2397–2406.
[25] G. P. Agrawal, "Nonlinear fiber optics," in *Nonlinear Science at the Dawn of the 21st Century*. Berlin, Germany, Springer, 2000, pp. 195–211.
[26] C. Häger and H. D. Pfister, "Physics-based deep learning for fiber-optic communication systems," *IEEE J. Sel. Areas Commun.*, vol. 39, no. 1, pp. 280–294, Jan. 2021, doi: 10.1109/JSAC.2020.3036950.
[27] F. J. García-Gómez and G. Kramer, "Mismatched models to lower bound the capacity of dual-polarization optical fiber channels," *J. Lightw. Technol.*, vol. 39, no. 11, pp. 3390–3399, Jun. 2021, doi: 10.1109/JLT.2021.3069686.
[28] E. Giacoumidis et al., "Comparison of DSP-based nonlinear equalizers for intra-channel nonlinearity compensation in coherent optical OFDM," *Opt. Lett.*, vol. 41, no. 11, pp. 2509–2512, May 2016, doi: 10.1364/OL.41.002509.
[29] Z. Zhou, "Clustering," in *Machine Learning*, 1st ed. Beijing, China: Tsinghua Univ. Press, 2016, pp. 197–201.
[30] S. Anees and M. R. Bhatnagar, "Performance evaluation of decode-and-forward dual-hop asymmetric radio frequency-free space optical communication system," *Inst. Eng. Technol. Optoelectron.*, vol. 9, no. 5, pp. 232–240, Oct. 2015, doi: 10.1049/iet-opt.2014.0118.